

Latent Catalyst-Containing Naphthoxazine: Synthesis and Effects on Ring-Opening Polymerization

Wenfei Zhang,^{†,‡} Pablo Froimowicz,^{*,†,§} Carlos R. Arza,[†] Seishi Ohashi,[†] Zhong Xin,[‡] and Hatsuo Ishida^{*,†}

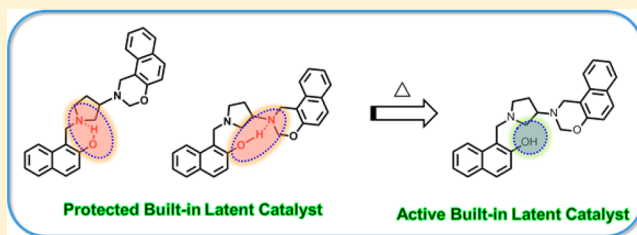
[†]Department of Macromolecular Science and Engineering, Case Western Reserve University, Cleveland, Ohio 44106-7202, United States

[‡]Shanghai Key Laboratory of Multiphase Materials Chemical Engineering, State Key Laboratory of Chemical Engineering, School of Chemical Engineering, East China University of Science and Technology, 130 Meilong Road, Xuhui District, Shanghai 200237, People's Republic of China

[§]Design and Chemistry of Macromolecules Group, Institute of Technology in Polymers and Nanotechnology (ITPN), UBA-CONICET, School of Engineering, University of Buenos Aires, Las Heras 2214 (CP 1127AAR), Buenos Aires, Argentina

S Supporting Information

ABSTRACT: A naphthoxazine containing a latent catalyst based on $-OH$ as part of its monomer structure has been synthesized through a simple one-pot reaction at room temperature. The chemical structure of this naphthoxazine monomer has been confirmed by 1H NMR, ^{13}C NMR, and FT-IR and its purity by elemental analysis. Differential scanning calorimetry (DSC) and *in situ* FT-IR have been used to investigate the active and inactive conditions for the latent catalysis. DSC and thermogravimetric analysis (TGA) studies indicate that this naphthoxazine polymerizes quickly before the monomer evaporation, as is often the case for conventional naphthoxazines, minimizing the monomer loss during polymerization. The intramolecular interactions between the $-OH$ group and oxazine ring and pyrrolidine ring of the monomer have been investigated in detail by using the homonuclear two-dimensional (2D) NMR technique $^1H-^1H$ nuclear Overhauser effect spectroscopy (NOESY). The $-OH$ interacts with the N in the pyrrolidine ring and oxazine ring through stable intramolecular hydrogen bonds instead of presenting free $-OH$ at room temperature, leading to the enhanced shelf life of the monomer. The free phenolic $-OH$ initiates and catalyzes the polymerization once the hydrogen-bonded interactions are weakened or disrupted upon increasing temperature, showing a latent catalytic effect.



INTRODUCTION

Polybenzoxazine, as a relatively new type of thermoset resin, has aroused much scientific research interest.^{1–4} Specifically, this class of resins offers significant merits in high thermal resistance,⁵ near-zero shrinkage upon polymerization,^{6,7} flexible molecular design capability,⁸ low flammability,^{9,10} and low surface free energy.^{11,12} Among these polybenzoxazine resins, naphthoxazines synthesized from naphthol, primary amines, and formaldehyde are expected to exhibit higher char yield than benzoxazines from phenol in that naphthoxazine polymers contain polynuclear aromatic structures which are known to exhibit excellent thermal stability because of the double bond conjugation.^{13–16} In addition, it is at the room temperature that naphthoxazine can be obtained, which is much more preferable than phenol-related benzoxazine since it is generally synthesized at the reflux temperature of the solvent used.² Higher temperature synthesis tends to produce oligomers that are difficult to be eliminated during the purification process.

The polymerization reaction of naphthoxazines and benzoxazines takes place without added initiators and/or catalysts,

though the polymerization rate can be accelerated by adding those compounds. The exothermic peak temperature corresponding to naphthoxazine and benzoxazine polymerization is in the range of 200–270 °C,^{15–17} but naphthoxazines usually evaporate more than benzoxazines before or during polymerization,^{13–15} causing serious monomer loss. In order to alleviate this instability, naphthoxazines have been modified by the introduction of another curable group or polynuclear forming aromatic structures,^{13–15} showing a useful approach to develop polynaphthoxazines with better thermal performance. For instance, Ishida and co-workers have synthesized a series of naphthoxazines from different hydroxynaphthalenes such as 1-naphthol, 2-naphthol, and 1,5-dihydroxynaphthalene with amine and formaldehyde. As reported, aniline has been served as an aromatic structure,¹³ while allylamine,¹⁴ alkylamine,¹⁸ and cyanate ester functionalized primary amine curable groups¹⁶

Received: June 2, 2016

Revised: September 2, 2016

Published: September 22, 2016



are also used. It has been found that the polymerization of allyl-containing and cyanate ester functional naphthoxazine monomer shows two exotherms at different temperature ranges, owing to the polymerization of allyl group (or cyanate ester trimerization) and the ring-opening polymerization of oxazine ring, respectively. The presence of a suitable reactive group into naphthoxazines is beneficial to increase the reactivity of naphthoxazines, which is going to increase the cross-link density as well as thermal stability. However, Uyar et al. have reported that evaporation and degradation of naphthoxazines based on aromatic amines are still detected during its polymerization process.¹⁵ Moreover, those alkyl-functional naphthoxazine monomers are also subjected to evaporation and degradation during the polymerization process.¹⁸ The common observation from these reports is that evaporation and degradation before or during the polymerization indicates the difficulty of their polymerization process as well as the undesired monomer loss despite the potential benefits of high char yield and thermal stability of the polymer. Therefore, carefully designed systems that alleviate these difficulties must be developed and evaluated.

Adding an initiator and/or catalyst to the naphthoxazine is a valid approach to achieve this goal. Various initiators, such as phenol,¹⁹ carboxylic acid,¹⁹ and many other cationic initiators,^{16,20} have been added to benzoxazine systems to accelerate the polymerization. However, insolubility of some of the initiators and/or catalysts into the benzoxazine resin, shortening of the shelf life by the added initiator and/or catalyst if it is mixed homogeneously, lack of the effectiveness of the intermolecularly added initiator/catalyst, and influence on the properties of the resulting polymer by the additive all make intermolecularly administrated initiators/catalyst unattractive. Some catalytically active groups have also been built in benzoxazine itself.^{20–22} Kiskan et al. have synthesized hydroxyethyl-terminated ether chain-functional benzoxazine monomers and found that the polymerization has been accelerated.²¹ Kudoh et al. subsequently studied the mechanistic role of hydroxyethyl group in activating the polymerization of hydroxyethyl functional benzoxazines.²² It was found that this compound shows higher polymerization rate accounting for the intramolecular interaction of the –OH group with cationic moieties of the zwitterionic intermediates formed by the ring-opening reaction of benzoxazine. Moreover, Baqar et al. have investigated the polymerization mechanism of methylol functional benzoxazine monomers synthesized via a condensation reaction of *o*-, *m*-, or *p*-methylolphenol, aniline, and paraformaldehyde.²⁰ They have demonstrated that the highest reactivity of methylol monomer is attributed to the catalytic effect of methylol group on the ring-opening due to the intramolecular hydrogen bond between the methylol and the oxygen in the opened oxazine ring. Although the reported works above show increased polymerization rate which decreases the monomer evaporation to a great extent, the stability of monomer needs to be enhanced in the future because the built-in of catalytically active group in benzoxazine or naphthoxazine will disrupt its stability and shorten the shelf life.

To overcome the limitations, herein, a built-in latent catalyst based on an –OH group is introduced in naphthoxazine. Specifically, the –OH group is placed at the 2-position of the naphthalene ring, whereas the substitution on the ring occurs at the 1-position. The well-designed –OH-containing naphthoxazine structure is expected to form intramolecular hydrogen

bonds as a stable latent form, which enhances the shelf life of naphthoxazine. Once the stable latent form is broken by increasing temperature, free catalytic –OH is generated and triggers the polymerization to proceed quickly. Understanding the structure and role of the intramolecular hydrogen bonding in benzoxazine monomers and polybenzoxazines has been the subject of active investigation.^{23–26} The detailed interaction between the –OH group and the neighboring protons, which allows the identification of the different interactions, has been investigated by two-dimensional (2D) ¹H–¹H nuclear Overhauser effect (NOESY) NMR spectroscopy.

EXPERIMENTAL SECTION

Materials. 2-Naphthol (99%), formaldehyde solution (37 wt % in water), and 3-aminopyrrolidine dihydrochloride (98%) were purchased from Sigma-Aldrich. Anhydrous ethanol (99.9%), chloroform (99.9%), hexanes (99%), molecule sieves (0.3 nm), and sodium hydroxide were purchased from Fisher Scientific. All the chemicals were used as received except for the deuterated solvent (DMSO-*d*₆) which was dried over molecular sieves for more than 2 days until there was no water signal observed in the NMR spectrum.

Synthesis of 1-((3-(1H-Naphtho[1,2-*e*][1,3]oxazin-2(3H)-yl)-pyrrolidine-1-yl)methyl). Naphthalene-2-ol (Abbreviated as NN-pd-OH). Prior to the synthesis, pyrrolidiamine-2HCl was pretreated by adding 2 mM sodium hydroxide solution in an ice bath. Afterward, formaldehyde (37 wt % in H₂O, 3.0 mmol) and neutralized pyrrolidiamine (1.0 mmol) were added into a solution of 2-naphthol (2.0 mmol) in chloroform (20 mL), which have molecular sieves. The reaction system was stirred at room temperature for 2 h. Then, the chloroform was mostly evaporated under air flow at room temperature. The crude product was dissolved in chloroform (5 mL) again, and it was dropped into hexanes (100 mL) where the naphthoxazines precipitated out of the solvent. The obtained white powder was recrystallized from ethanol yielding white crystals (yield: 71%). ¹H NMR (600 MHz, DMSO-*d*₆, ppm): δ = 1.82–2.05 (m, 2H; CH₂–CH₂–CH), 2.65–2.71 (m, N–CH₂–CH₂), 2.71–2.92 (m, 2H; N–CH₂–CH), 3.56 (m, 1H; CH₂–CH–CH₂) 4.13 (t, 2H; Ar–CH₂–N), 4.29 (dd, 2H; Ar–CH₂–N, oxazine), 4.90 ppm (dd, 2H; O–CH₂–N, oxazine), 7.01 (d, 1H), 7.06 (d, 1H), 7.26 (t, 1H), 7.37 (t, 1H), 7.40 (t, 1H), 7.48 (t, 1H), 7.68 (d, 3H, overlapped), 7.76 (d, 1H), 7.83 (d, 1H), 7.94 (d, 1H). ¹³C NMR (600 MHz, DMSO-*d*₆, ppm): δ = 29.8, 45.6, 51.9, 52.8, 58.3, 58.6, 81.3, 113.1, 113.8, 118.6, 118.9, 121.7, 122.6, 122.7, 123.7, 126.4, 126.9, 128.0, 128.4, 128.7, 128.8, 128.9, 129.0, 131.7, 133.3, 152.6, 155.4. FT-IR (KBr): ν = 1227 cm^{–1} (C–O–C asymmetric stretching), 1139 cm^{–1} (C–N–C asymmetric stretching), 924 cm^{–1} (the benzoxazine-related mode). Elemental analysis (C₂₇H₂₆N₂O₂): Calcd C 79.00, H 6.38, N 6.62. Found C 78.44, H 6.45, N 6.95. Purity: 99.30%.

Latent Catalytic Effect and Mechanism Study. The latent catalytic effect during the polymerization of NN-pd-OH was carefully investigated by using *in situ* FT-IR, DSC, and TGA. In detail, NN-pd-OH monomer was dissolved in methylene chloride with a concentration of 100 mM, and subsequently a thin film was cast on a KBr plate. Once the solvent was totally evaporated, the naphthoxazine film was sandwiched by another KBr plate to prevent the material flow during melting and minimize the evaporation of the monomer. The as-prepared sample was placed into a heating cell and heated from room temperature to 220 °C at a heating rate of 5 °C/min. In addition, DSC analysis was conducted to obtain complementary information on the latent catalytic effect at the heating rate of 5 °C/min from room temperature to 300 °C under a nitrogen atmosphere. TGA was utilized to study the thermal behavior of NN-pd-OH at the heating rate of 5 °C/min from room temperature to 800 °C under a nitrogen atmosphere. It must be mentioned that *in situ* FT-IR, DSC, and TGA studies were processed at the same heating rate to ensure that the results of every analysis are comparable. Furthermore, a control experiment comparing the behavior between our resin containing the built-in catalyst and a system formed with a

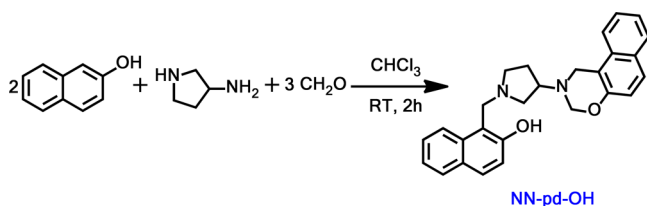
naphthoxazine and a very similar external catalyst has been carried out as “a blank experiment”. Specifically, a similar naphthoxazine without the $-OH$ group (N-m, Figure S1) and 2-naphthol as an external catalyst were mixed homogeneously in a molar ratio of 1:1. Therefore, the stoichiometric ratio of OH to oxazine ring in this mixture is the same as that in NN-pd-OH. Initially, both compounds, N-m (1 mmol) and 2-naphthol, were dissolved completely in $CHCl_3$ (3 mL). The two solutions were then mixed drop by drop with magnetic stirring, ensuring homogeneous mixture at the molecular level. Afterward, the solvent was evaporated under gentle air flow and then dried overnight in a vacuum oven. The obtained mixture was denoted as N-m/2N. Then, a series of DSC and 1H NMR analysis of the two systems, NN-pd-OH and N-m/2N, were carried out. NN-pd-OH and N-m/2N were heated in solid state at 60 and 100 $^{\circ}C$ for 1 h, respectively. 1H NMR was used to obtain complementary information on chemical structure and compositions of NN-pd-OH as well as for N-m/2N. The mechanism of this latent catalytic effect was studied by 2D 1H - 1H NMR NOESY. The 3D structure of NN-pd-OH was drawn using Chem3D 15.0.

Characterization. The chemical structure of NN-pd-OH was confirmed by 1D 1H NMR in $DMSO-d_6$ on a Varian Oxford AS600 at a proton frequency of 600 MHz. The relaxation time used for the integration of the resonances was 10 s. The ^{13}C NMR spectrum was also acquired in $DMSO-d_6$ at a carbon frequency of 150.864 MHz. The average number of transients for 1H and ^{13}C NMR was 8 and 512, respectively. The chemical structure was further confirmed by a Bomem Michelson MB100 FT-IR spectrophotometer. The spectrophotometer was equipped with a deuterated triglycine sulfate detector. A solution of NN-pd-OH monomer in methylene chloride was used to cast a thin film onto a KBr plate. After purging the spectrometer with dry air for 30 min, the spectra were collected at a resolution of 4 cm^{-1} in the range of 4000 – 500 cm^{-1} at room temperature. Elemental analysis was conducted with PerkinElmer 2400 Series II CHNS/O Analyzer at Galbraith Laboratories, Inc. Moreover, a TA Instruments DSC model 2920 was utilized with a heating rate of $5\text{ }^{\circ}C/\text{min}$ and a nitrogen flow rate of $60\text{ mL}/\text{min}$ for the differential scanning calorimetric (DSC) study. To calculate the activation energy of NN-pd-OH polymerization, the samples ($1.5 \pm 0.5\text{ mg}$) were analyzed at different heating rates of 2, 5, 10, 15, and $20\text{ }^{\circ}C\text{ min}^{-1}$. All samples were sealed in hermetic aluminum pans with lids. The reactivity study of NN-pd-OH monomer was accomplished by obtaining isothermal FT-IR spectra on a Bomem Michelson MB100 FTIR spectrophotometer. Eight scans were recorded at a resolution of 4 cm^{-1} . Sample was inserted into a hot cell which was adapted to the FT-IR spectrometer, and the experiment begun as soon as the hot cell temperature reached the desired temperature (100, 130, and $160\text{ }^{\circ}C$), which took 2 min. The 2D 1H - 1H NOESY NMR experiment was carried out in $DMSO-d_6$ with tetramethylsilane as an internal standard on a Varian Oxford AS600 at a proton frequency of 600 MHz. Typically, parameters used in the 2D NMR experiments were as follows: 2048 data points along the f_2 dimension, 256 free induction decays in the f_1 dimension, number of scans 16, relaxation delay 2 s, and mixing time 900 ms in this work. Experiments were performed at room temperature.

RESULTS AND DISCUSSION

Synthesis of NN-pd-OH. As shown in Scheme 1, naphthol group-containing naphthoxazine monomer has been synthe-

Scheme 1. Synthesis Procedure of NN-pd-OH



sized using 2-naphthoxazine, pyrrolidiamine, and formaldehyde as starting materials. Typically, phenolic hydroxyl group-containing benzoxazine is difficult to synthesize through one-pot Mannich reaction because of the presence of two different hydroxyl groups (one is for forming oxazine ring, and the other one is the free $-OH$ group), and extra acid catalyst should generally be added into the reaction system to control and maintain one of the two hydroxyl groups unreacted. In addition, each reaction step for synthesizing hydroxyl group-containing benzoxazine needs careful temperature control, especially for benzoxazine ring closure.

Naphthol has been reported to exhibit higher reactivity than ordinary phenols due to its extra electron-rich benzene ring.¹⁶ Based on its high reactivity, NN-pd-OH has been obtained according to a low energy-consuming one-step Mannich reaction at room temperature, alleviating side reactions or byproducts caused by the heating process. The NN-pd-OH monomer is obtained as white crystals, and the reaction yield is 71%.

The chemical structure of NN-pd-OH has been confirmed by 1H NMR. As shown in Figure 1, two quintuplet resonances located at 4.29 and 4.90 ppm are attributed to the $Ar-CH_2-N$ and $O-CH_2-N$ of the oxazine ring, respectively, proving naphthoxazine ring formation. It should be noted that the splitting of these two signals is not very common in oxazine rings. From the aspect of the molecule and possible conformations, the existence of rigid and stiff structures trapped by some intramolecular interactions, such as the proposed intramolecular hydrogen bond. These interactions involving the pyrrolidine ring, the oxazine ring, and the aromatic rings can easily cause the observed splitting of the signals for protons in positions f and g since they cannot experience free rotation, thus making the germinal protons different. One singlet resonance located at 4.13 ppm corresponds to the $Ar-CH_2-N$ shown as H_a in Figure 1 between naphthol and pyrrolidine. The rest of the resonances located in the range of 1.82–3.56 ppm are the signals related to the protons of pyrrolidine ring.

Additionally, the ^{13}C NMR spectrum shown in Figure 2 is useful to identify the characteristic signal of oxazine and pyrrolidine rings. The resonances at 58.6 and 81.3 ppm are consistent with the reported signals attributed to $Ar-CH_2-N$ and $O-CH_2-N$ of the oxazine ring.¹⁶

It should be mentioned that DMSO is a stronger hydrogen-bonding acceptor than chloroform.²⁶ Thus, DMSO forms strong interaction with the $-OH$ proton from NN-pd-OH, slowing the exchange rate of the proton and, thus, making it visible by NMR. Although the signal may be visible, it is not integrable since the proton exchange still exists. Interestingly, it seems that the proton of $-OH$ group of NN-pd-OH in this 1H NMR study has not been observed when $DMSO-d_6$ is the solvent. This might be either because the signal for $-OH$ is overlapped or not detected. To further study whether the signal of $-OH$ is overlapped (or not detected), deuterated water (D_2O) was added into the NMR sample. The proton in $-OH$ will exchange with a deuteron from the D_2O . It should be mentioned that the signal for DOH shifts once the amount of added D_2O changes as shown in Figure S2. Herein, for a detailed study, 0.1 mL of D_2O was added into the NN-pd-OH NMR sample in which the content of $DMSO-d_6$ is 0.8 mL. As a reference, 0.1 mL of D_2O was added into 0.8 mL of $DMSO-d_6$ without NN-pd-OH. Figure 3 shows the 1H NMR spectra of NN-pd-OH in $DMSO-d_6$ before and after adding D_2O . After

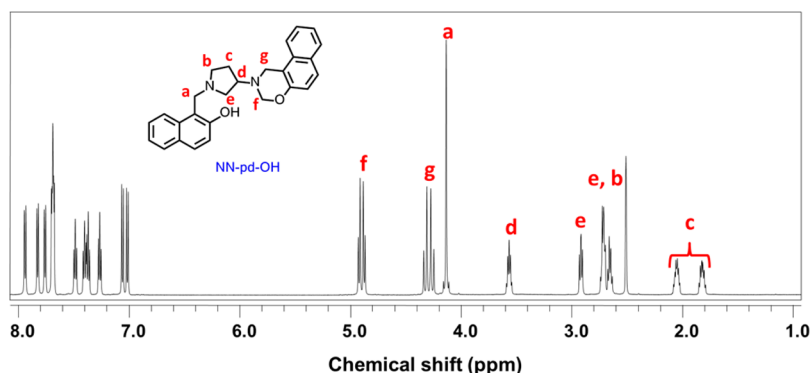


Figure 1. ^1H NMR spectrum of NN-pd-OH in extremely dried $\text{DMSO}-d_6$.

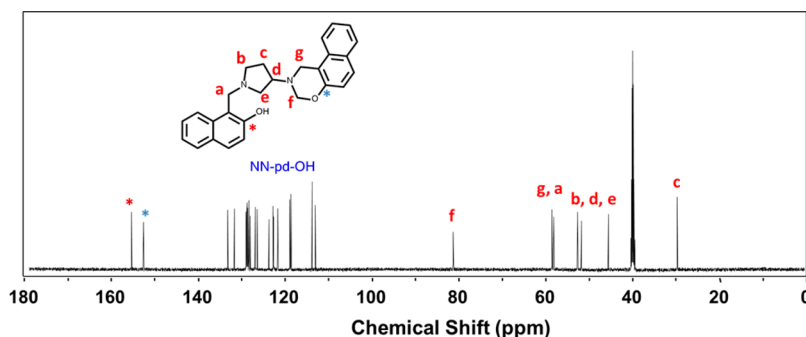


Figure 2. ^{13}C NMR spectrum of NN-pd-OH in $\text{DMSO}-d_6$.

the addition of D_2O , shape and integration value of the complex signal at 7.68 ppm decreases by 0.25 as shown in Figure 3b. Meanwhile, the signal integration for DOH at 3.76 ppm increases from 4.67 to 5.70 as shown in Figure 3c. The blue spectrum is that of 0.1 mL of D_2O in $\text{DMSO}-d_6$. The increment of 1.03 is due to the exchange from active hydrogen ($-\text{OH}$) to DOH after D_2O was added. Therefore, signal for protons of the $-\text{OH}$ group overlaps with that of three aromatic protons at 7.68 ppm. Moreover, integration decrease (0.25) at 7.68 ppm is less than the integration increase (1.03) at 3.76 ppm, which is due to the signal for $-\text{OH}$ -forming intramolecular hydrogen bonds at 11.32 ppm even in $\text{DMSO}-d_6$ as shown in Figure S3.

To further verify the chemical structure of NN-pd-OH, FT-IR analysis has been performed, and the results are shown in Figure 4. IR spectroscopy has become a standard method to investigate hydrogen bonds in the solid state.²⁷ Intramolecular hydrogen bonds in benzoxazine systems typically appear as a broad band in the range between 2600 and 3000 cm^{-1} . The spectrum of NN-pd-OH shows this band. At the same time, there is no obvious peak corresponding to free $-\text{OH}$ appearing around 3100–3600 cm^{-1} . These results suggest that most of $-\text{OH}$ are intramolecularly hydrogen-bonded. Additionally, it is reasonable that free $-\text{OH}$ signals cannot be observed obviously in the IR spectra. It has been reported that IR spectra of $-\text{OH}$ -containing asymmetric methyl dimer (benzoxazine model compound) in liquid phase and solution state show no signal for free $-\text{OH}$ or intermolecular hydrogen bonded $-\text{OH}$ at 3100–3600 cm^{-1} , but the signal for intramolecular hydrogen bonds at 2750 cm^{-1} .²⁸ Thus, the FT-IR spectrum in solid state shows mostly intramolecular hydrogen bonds as a broad band at 2600–3000 cm^{-1} in this work because the molecule in the crystal state is easier to form intramolecular interactions than in the solution state. All of the results demonstrate the existence

of $-\text{OH}$. Moreover, the bands at 1227, 1139, and 924 cm^{-1} are attributed to the $\text{C}-\text{O}-\text{C}$ asymmetric stretching, $\text{C}-\text{N}-\text{C}$ asymmetric stretching, and benzoxazine-related band, respectively, demonstrating the formation of naphthoxazine.

Polymerization Behavior of NN-pd-OH and the Latent Effect. The polymerization behavior of naphthoxazine monomer has been investigated by DSC. A thermogram of NN-pd-OH is shown in Figure 5. As can be seen in the figure, there is one exothermic peak with maximum at 183 $^{\circ}\text{C}$ and an onset temperature of about 171 $^{\circ}\text{C}$. This process is related to the polymerization of the naphthoxazine monomer. The exothermic peak temperature of NN-pd-OH is lower than that of other naphthoxazines reported before such as 206 $^{\circ}\text{C}$ for naphthoxazine functionalized with a cyanate ester group¹⁶ or 214 $^{\circ}\text{C}$ for aromatic amine-based naphthoxazine.¹³ NN-pd-OH is present in the form of pure needle crystals, which melting is observed as a sharp endothermic peak in DSC thermogram at 123 $^{\circ}\text{C}$. The actual half-width of this melting peak is calculated from the original data and is 4.8 $^{\circ}\text{C}$, which shows a melting range between 124.5 and 119.8 $^{\circ}\text{C}$ for about 2 mg of sample. This range is narrow and very reproducible, demonstrating the high purity of NN-pd-OH. Since it shows a relatively sharp and clear melting endotherm for the naphthoxazine crystal, this reduction of the polymerization temperature is not due to the impurities, but instead to some inner interaction within the NN-pd-OH molecule itself.

The polymerization kinetics of NN-pd-OH has been studied with nonisothermal DSC at different heating rates of 2, 5, 10, 15, and 20 $^{\circ}\text{C}/\text{min}$ as shown in Figure 6. The apparent activation energy of the polymerization process has been calculated according to the well-known Kissinger and Ozawa methods.^{29,30} Based on the Kissinger method, the activation energy (E_a) can be calculated using eq 1 as follows:

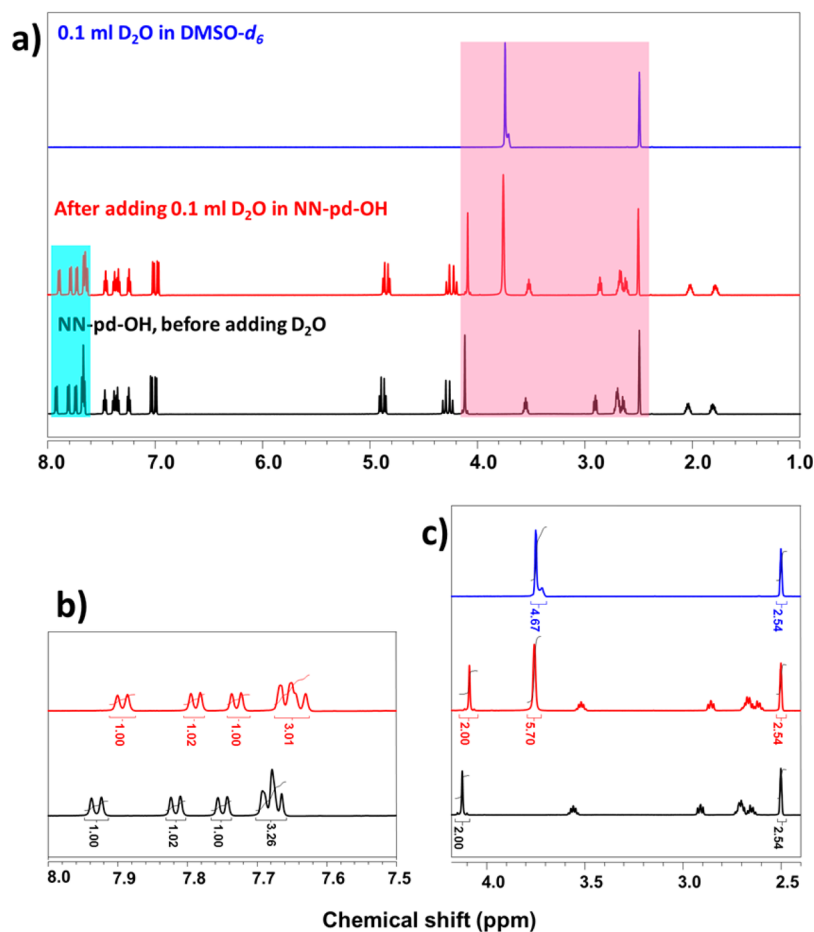


Figure 3. ^1H NMR spectra of 0.1 mL of D_2O in $\text{DMSO}-d_6$ (in blue) and NN-pd-OH at a concentration of 35 mM in $\text{DMSO}-d_6$ before (in black) and after adding 0.1 mL of D_2O (in red). (a) Full spectra. (b) Magnification of the region between 7.5 and 8.0 ppm, highlighted in blue in (a). (c) Magnification of the region between 2.4 and 4.2 ppm, highlighted in red in (a). Each sample has 0.8 mL of $\text{DMSO}-d_6$.

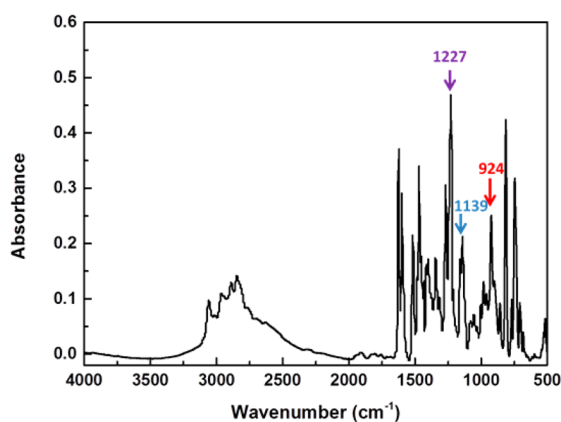


Figure 4. FT-IR spectrum of NN-pd-OH monomer.

$$\ln \frac{\beta}{T_p^2} = \ln \frac{AR}{E_a} - \frac{E_a}{RT_p} \quad (1)$$

where β is the heating rate, T_p is the exothermic peak temperature, A is the frequency factor, R is the gas constant, and E_a is the activation energy. For the Ozawa method, the activation energy can be determined using eq 2:

$$\ln \beta = -1.052 \frac{E_a}{RT_p} + C \quad (2)$$

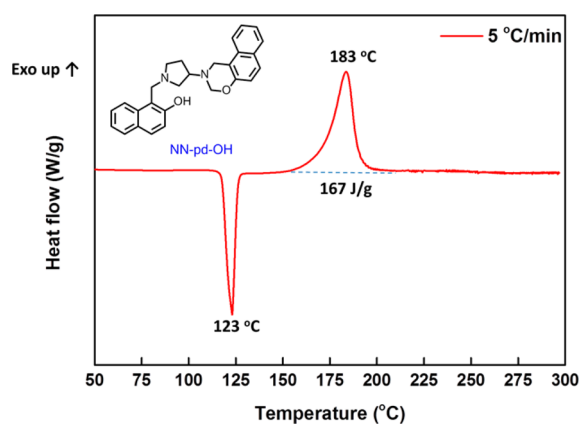


Figure 5. DSC thermogram of NN-pd-OH at a heating rate of 5 °C/min.

where C is a constant.

Alternatively, E_a can be obtained graphically using these equations. If the plots of $\ln(\beta/T_p^2)$ and $\ln \beta$ against $1/T_p$ are linear, a single process can be assumed, and the corresponding E_a can be obtained from the slope of the straight line.

Figure 7 illustrates the plots of $\ln(\beta/T_p^2)$ and $\ln \beta$ against $1/T_p$ according to the Kissinger and Ozawa method, respectively. The activation energy is calculated to be 107.2 and 109.2 kJ/mol by using the Kissinger and Ozawa methods, respectively.

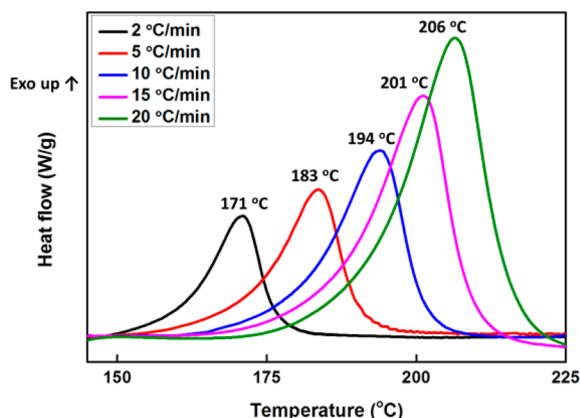


Figure 6. DSC curves of NN-pd-OH at various heating rates.

This estimated activation energy is lower than that of some reported asymmetric benzoxazines, such as 169 kJ/mol (Kissinger) for amide-functional benzoxazine and 247 kJ/mol (Kissinger) for imide-functional benzoxazine.³¹ It is also lower than that of classic benzoxazines without a built-in catalyst, such as 116 kJ/mol (Ozawa) for monofunctional benzoxazine.³² These results suggest that NN-pd-OH is easy to be activated to polymerize.

Nevertheless, the relatively low polymerization temperature or low activation energy is not the most attractive aspect of this work. To gain deeper understanding, *in situ* FT-IR has been utilized to study its polymerization behavior. The KBr plate with a thin NN-pd-OH film on the surface has been carefully sandwiched to avoid evaporation and flow of the melt, and spectra have been collected at a certain interval at the heating rate of 5 °C/min. Results are shown in Figure 8. The peak intensity at 924 cm⁻¹ against temperature has been plotted (in blue) together with the DSC curve (in red) and TGA curve (in black) at the same heating rate of 5 °C/min. As shown in Figure 9, on one hand, the steepest intensity reduction of the benzoxazine related band at 924 cm⁻¹ of NN-pd-OH coincides with the melting endothermic peak in the DSC thermogram. This indicates that the rate of oxazine ring-opening suddenly increases as soon as the NN-pd-OH crystals melt. It should be pointed out that the intensity reduction of the 924 cm⁻¹ band does not necessarily mean the polymerization of naphthoxazine but corresponds to the opening of the oxazine ring. On the other hand, it can be clearly seen from the TGA curve (in

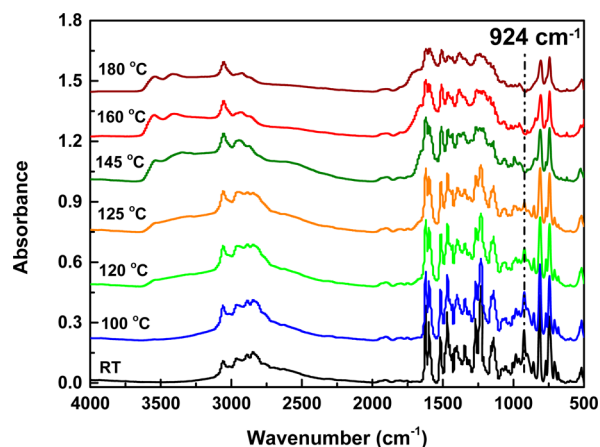


Figure 8. Representative *in situ* FT-IR spectra of NN-pd-OH at various temperatures with a constant heating rate of 5 °C/min.

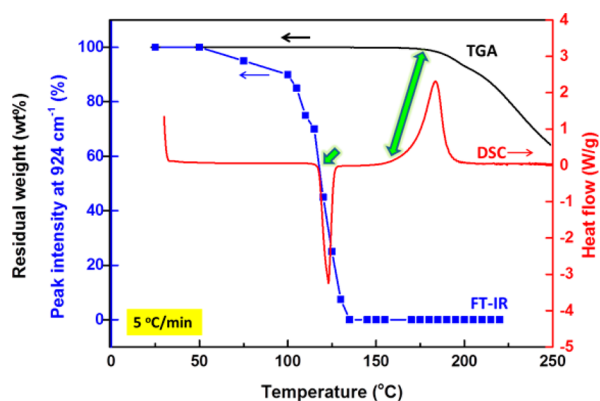


Figure 9. Variation in IR peak intensity at 924 cm⁻¹ (in blue), TGA (in black), and DSC thermogram (in red) upon increasing of temperature. All three results have been obtained at the same heating rate of 5 °C/min.

black) that the onset degradation temperature of naphthoxazine monomer does not start until around 170 °C. Thus, the IR intensity reduction is not caused by the material loss, but due to the ring-opening reaction of the oxazine ring. That is to say, the ring-opening polymerization of NN-pd-OH happens before the monomer loss caused by the evaporation or degradation. It is hypothesized that there is an inner interaction effect to stabilize the NN-pd-OH monomer before it starts to polymerized,

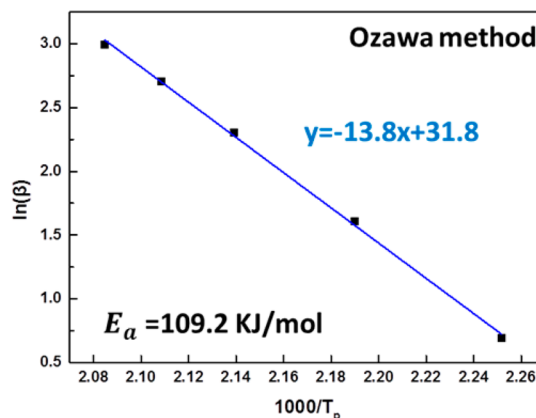
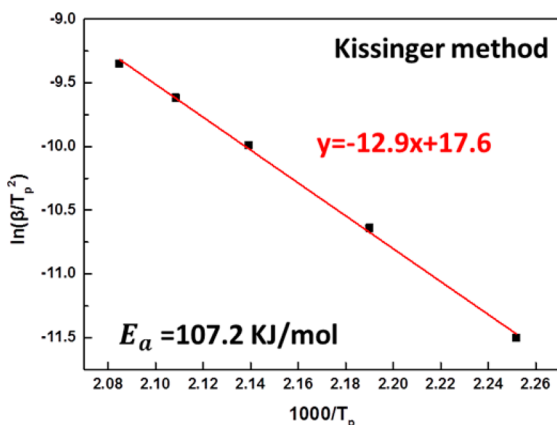


Figure 7. Plots generated following the Kissinger and Ozawa methods for determination of the activation energy of NN-pd-OH.

which is regarded as the latent effect. It is also interesting to note that there is a large discrepancy between the ring-opening temperature as shown by the IR intensity reduction of the 924 cm^{-1} centered around $123\text{ }^{\circ}\text{C}$ and the polymerization as observed by the DSC exothermic peak at $183\text{ }^{\circ}\text{C}$. Such a discrepancy between the ring-opening and polymerization has been reported by Dunkers et al. using dielectric constant measurement on the benzoxazine monomer based on *p*-cresol and methylamine.¹⁹

A control experiment has also been carried out to evaluate the latent effect and stability of the “built-in catalyst” NN-pd-OH. Thus, a mixture formed with N-m and 2N at the molar ratio of 1:1 was prepared. Therefore, the stoichiometric ratio of OH to oxazine ring in this system is the same as that in NN-pd-OH. Figure 10 shows the DSC thermograms of various samples

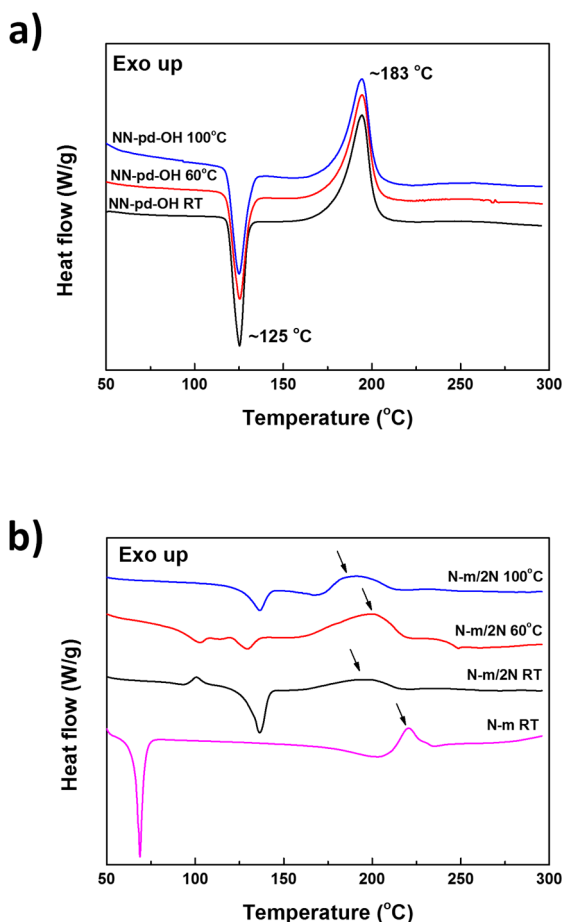


Figure 10. (a) DSC thermograms of NN-pd-OH (in black, bottom), the one pretreated at $60\text{ }^{\circ}\text{C}$ for 1 h (in red, middle), and that pretreated at $100\text{ }^{\circ}\text{C}$ for 1 h (blue, top). (b) DSC thermograms of N-m/2N (in black, second from the bottom), the one pretreated at $60\text{ }^{\circ}\text{C}$ for 1 h (in red, third from the bottom), and that pretreated at $100\text{ }^{\circ}\text{C}$ for 1 h (blue, top). The pink curve is the thermogram for N-m without added catalyst. Heating rate for the DSC study was $10\text{ }^{\circ}\text{C}/\text{min}$.

reflecting their thermal behavior. It can be seen in Figure 10a that even though the OH-containing NN-pd-OH has been treated at $100\text{ }^{\circ}\text{C}$ for 1 h, there is no chemical structural change during the heat treatment because all the DSC thermograms show the very same endothermic melting temperature ($\sim 125\text{ }^{\circ}\text{C}$) and exothermic polymerization temperature ($\sim 183\text{ }^{\circ}\text{C}$) as well as no new endothermic or exothermic peak is observed.

Moreover, in Figure S4, all signals for every proton in each sample have no variations in the ^1H NMR spectra, and no new signals are observed. This demonstrates the stability of NN-pd-OH when treated at $100\text{ }^{\circ}\text{C}$, which also indicates the latent effect. This “built-in latent catalyst” controls the polymerization of the naphthoxazine happening only after reaching a certain temperature, which will then trigger the reaction.

However, there is no “latent catalytic effect” in the N-m/2N system where an external OH-containing catalyst is added to an OH-free naphthoxazine. It has been reported that phenolic group-containing compound as an external catalyst reduces the polymerization of benzoxazines.³³ Expectedly, this phenomenon is also observed for the N-m/2N system. Both the stability and latent effect in N-m/2N are studied and compared in this work. In Figure 10b, DSC thermograms are different after each heating treatment since some new endothermic and/or exothermic peaks appear due to the thermal behavior of those new-generated compositions, which means the chemical composition of the N-m/2N mixture changes upon heating. For instance, the DSC curve shown in red is the sample preheated at $60\text{ }^{\circ}\text{C}$ for 1 h. A small endothermic peak can be seen at $\sim 105\text{ }^{\circ}\text{C}$, which possibly corresponds to the evaporation of small molecules generated during the heat treatment at $60\text{ }^{\circ}\text{C}$. N-m/2N, which is an external catalyst system, is not expected to have latent catalytic effect or be stable as the “built-in latent catalyst” compound NN-pd-OH. This conclusion has been further proved by combining the results from ^1H NMR study.

Figure S5 shows the ^1H NMR spectra of N-m (in purple), 2-naphthol (in purple), N-m/2N (in black), N-m/2N heated at $60\text{ }^{\circ}\text{C}$ for 1 h (in red), and that heated at $100\text{ }^{\circ}\text{C}$ for 1 h. Because of the free OH in 2-naphthol, there are some interactions happening when 2-naphthol is mixed with N-m. In view of ^1H NMR spectra, protons neighboring (or participating) these interactions can be influenced and exhibited changes (or new signals), e.g., signal at 2.24, 4.17, and 7.95 ppm in the ^1H NMR spectrum of N-m/2N at RT (shown in black). From the red spectrum in Figure S5, new peaks besides those for N-m and 2-naphthol in this mixture system are observed when N-m/2N is heated at $60\text{ }^{\circ}\text{C}$ for 1 h, especially in the range of 8.3–7.0 ppm. New peaks, such as peaks at 8.19, 7.65, 7.60, 7.18, 7.12, and 4.71 ppm marked with red arrows, are relatively stronger when N-m/2N is heated at $100\text{ }^{\circ}\text{C}$ for 1 h. This result is a solid evidence for the generation of new compositions in the N-m/2N system, showing the instability of the N-m/2N system. It should also be mentioned that the temperature of the pretreatment (60 and $100\text{ }^{\circ}\text{C}$) is much lower than the onset polymerization temperature for the system N-m/2N (around $165\text{ }^{\circ}\text{C}$ shown in Figure 10b). But there are reactions in the mixture below the onset polymerization temperature even at $60\text{ }^{\circ}\text{C}$, indicating the no “latent effect” of the external catalyst. It can be concluded by this comparison that the built-in catalyst in our naphthoxazine is stable and exhibits latent catalytic effect, which presents a novel concept for naphthoxazine. It is necessary to emphasize on the built-in structure since a simple mixing of naphthoxazine and external catalyst has no latent catalytic effect.

In addition, Figure 11 shows the conversion of NN-pd-OH monomer to ring-opening structure at various temperatures for 120 min, which was measured by following the normalized decrease in the area of the band at 924 cm^{-1} . Before the melting of NN-pd-OH monomer, the oxazine ring does not open too much at $100\text{ }^{\circ}\text{C}$ even for 120 min as shown in the

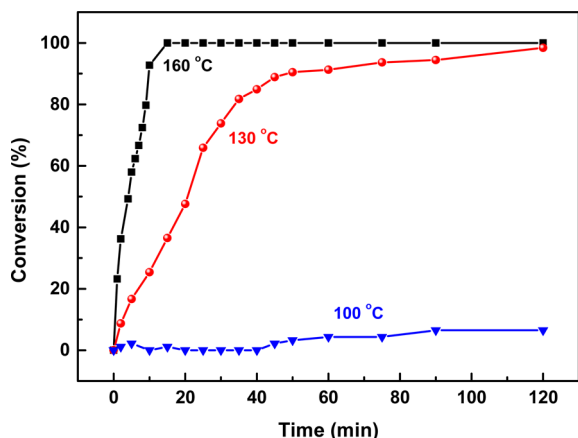


Figure 11. Conversions of oxazine ring-opening at 100, 130, and 160 °C for 120 min.

blue curve (triangle symbol). Once the monomer melted, oxazine ring opens rapidly, and the conversion reached 90% after polymerization for 50 min at 130 °C as illustrated in the red curve (closed circle). It is noteworthy that the oxazine ring opens completely only within 15 min at 160 °C, of which the reactivity is higher than reported benzoxazines such as those of isomeric bisphenol F and aniline-based 2,2', 2,4', and 4,4'-

substituted benzoxazine monomers.¹⁷ The conversion results are consistent with what has been observed in Figure 9, showing a catalytic effect and increasing the ring-opening polymerization rate.

NOESY Study. As mentioned in the Introduction, the hydroxyl group, whether covalently bonded to the monomeric benzoxazine molecule itself or physically mixed by adding an hydroxyl-containing compound to the benzoxazine, can catalyze the polymerization of benzoxazine in a way of decreasing the polymerization temperature. However, it is the latent-catalytic property that correlated to $-OH$ group is emphasized and differed in this work. Recently, Froimowicz et al. have utilized a powerful technique, 2D $^1H-^1H$ NOESY NMR spectroscopy, to determine the 3D structure of $-NH-$ substituted benzoxazine with intramolecular hydrogen bonds.²⁶ On the basis of those solid experimental results, they have concluded that the hydrogen-bonding system is responsible for the high reactivity of that benzoxazine toward polymerization. NOESY is a useful 2D $^1H-^1H$ NMR, which helps determining the interacting protons through space. The conformation of the monomer, in particular in the presence of hydrogen bonds involving the oxazine ring, strongly influences the rate of polymerization. Therefore, the objective in this section is to gain a deeper understanding of interactions in NN-pd-OH and relate them to the fast rate of ring-opening polymerization observed for NN-pd-OH.

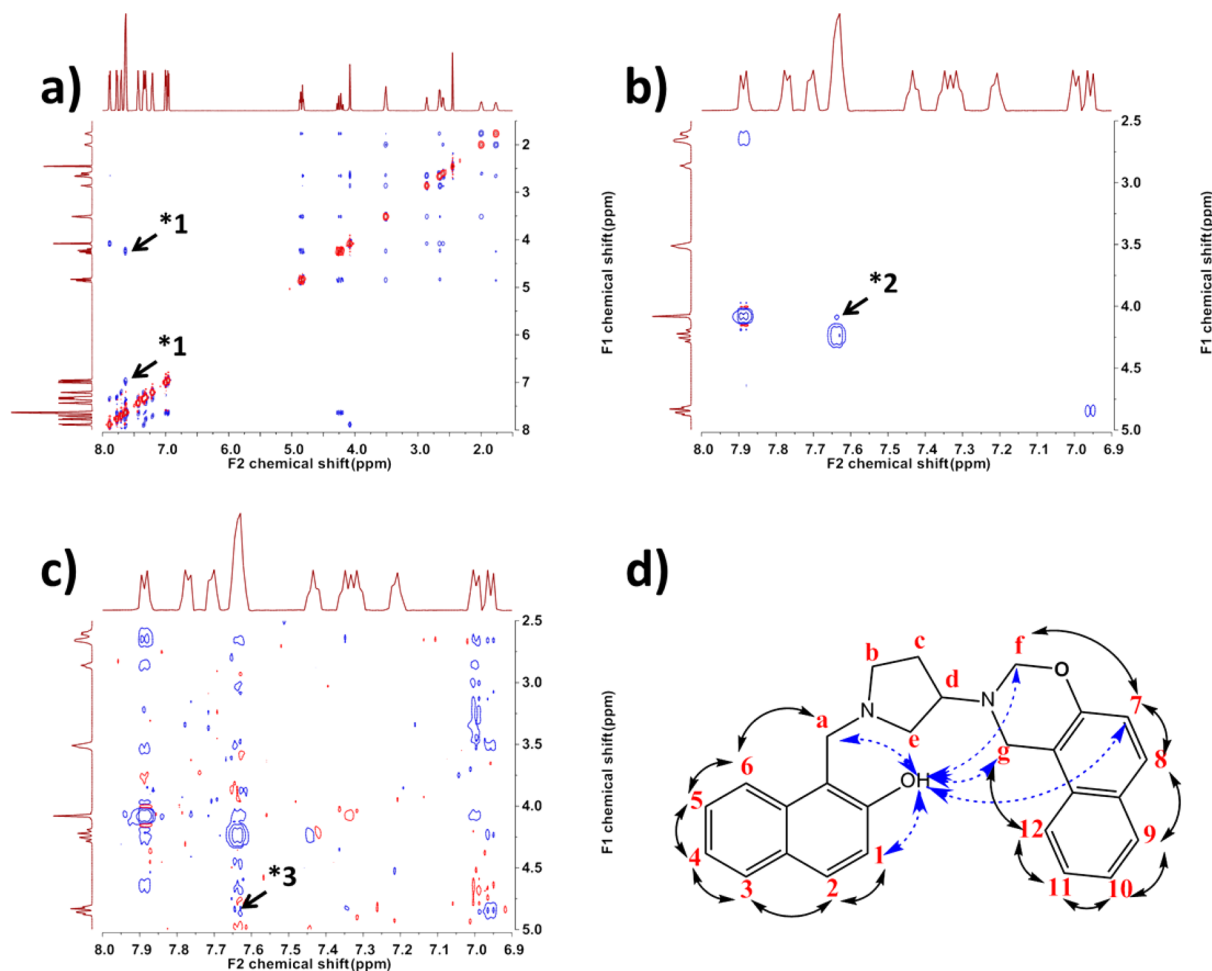


Figure 12. (a–c) 2D $^1H-^1H$ NMR spectra of NN-pd-OH in $DMSO-d_6$ and (d) summary of representative NOE interactions observed in the 2D $^1H-^1H$ NMR spectrum.

Prior to the NOESY study, the chemical shift of proton in OH group has been identified by the 1D ^1H NMR study as mentioned before and shown in Figure 2. Full and representative 2D ^1H – ^1H NMR spectra of NN-pd-OH in DMSO- d_6 are illustrated in Figure 12. Proton positions are labeled as shown in the chemical structure of NN-pd-OH in Figure 11d. By analyzing the through-space interactions between different protons in the NN-pd-OH molecule based on the 2D ^1H – ^1H NOESY NMR spectrum, it can be seen which protons from the entire molecule are indeed interacting with the –OH. As marked as *1 in Figure 12a, the signals represent through-space interactions between H_g and OH, H_1 and OH, and H_7 and OH. However, as mentioned before, the signal for OH overlaps with that of three other protons at 7.68 ppm, making it difficult to distinguish the through-space interaction between OH and H_g (or H_1 , H_7) from that between H_8 , H_9 , and H_{12} with the same –OH. Based on the detectable space distance range, one signal can be assigned to the through-space interactions between H_1 and OH since H_8 , H_9 , or H_{12} is much further away than 0.5 nm. To further interpret the through-space interactions, the phase corresponding to 2D ^1H – ^1H NMR has been lowered to observe the possible interactions related to OH. As marked as *2 in Figure 12b, the signal represents through-space interactions between H_a and H_8 , H_9 , or H_{12} . Since the through-space distance between H_a and H_8 , H_9 , H_{12} , or –OH is much further away than 1.0 nm, no NOE interaction should be observed. Therefore, it is concluded that this correlation should be assigned to be between OH and H_a . This result is also an additional evidence that the signal for –OH overlaps with those of H_8 , H_9 , and H_{12} . In addition, when the phase corresponding to 2D ^1H – ^1H NMR has been lowered more, a weak signal marked as *3 appeared in Figure 12c and is assigned to be the through-space interaction between H_f and OH. In summary, the general NOE interactions between protons in aromatic rings are marked with solid arrows, while the representative NOE interactions involving OH are marked with blue dotted arrows as shown in Figure 12d.

Upon these solid correlations observed from 2D ^1H – ^1H NOESY NMR spectra, the most probable 3D conformation of NN-pd-OH has been proposed as drawn in Figure 13a. If the left-side naphthalene is regarded right on the plane, the pyrrolidine ring shall be in the plane, while the oxazine ring and right-side naphthalene are out of the plane with angle less than 10° . In such a case, the distances between the proton in the –OH group and H_1 , H_a , H_g , H_b , and H_7 in Figure 13b are 0.30, 0.32, 0.37, 0.25, and 0.42 nm, respectively, which are in the detectable range for 2D ^1H – ^1H NOESY NMR spectroscopy. The structure hypothesized in Figure 13 makes the formation of intramolecular hydrogen bonds between the –OH group and N (or O) in oxazine ring (or in pyrrolidine ring) possible. The e^- lone pair in O might be delocalized with the electron cloud of naphthalene and might have a decreased electron density. Thus, an intramolecular hydrogen bond as $-\text{OH}\cdots\text{N}$ is more favorable. It has also been reported that there is internal six-membered ring involving hydrogen bonds between phenolic hydroxyl and methine nitrogen,³⁴ of which the chemical structure is similar to NN-pd-OH (within phenolic hydroxyl and pyrrolidine substitution).

The distance between –OH group and N in oxazine ring is about 0.23 nm, which is similar to that to N in the pyrrolidine ring. However, the electron density of N in oxazine ring is slightly lower than that of N in the pyrrolidine ring due to the slightly stronger electron-donating groups around N in the

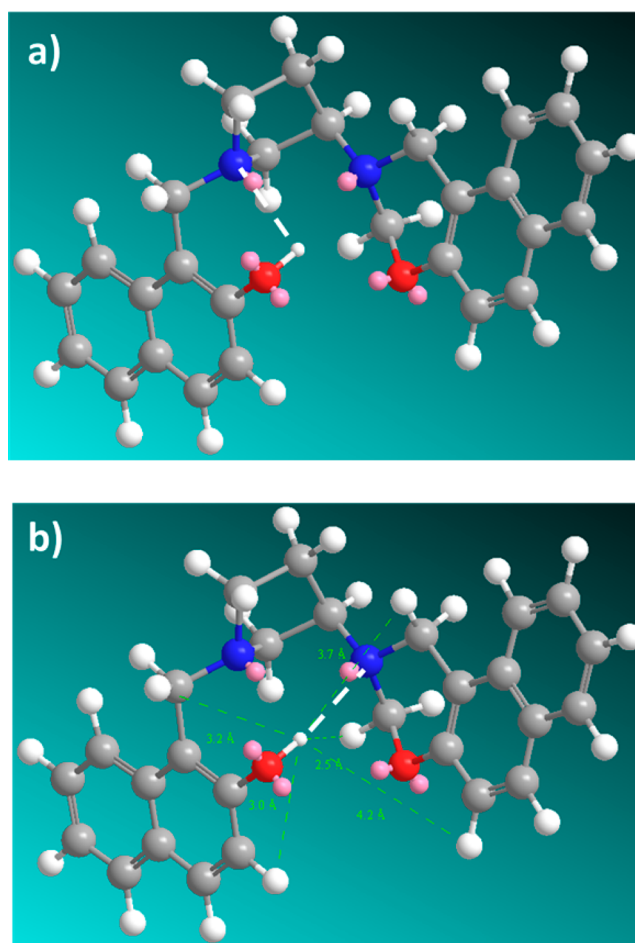


Figure 13. 3D structure and possible intramolecular hydrogen bonds in NN-pd-OH.

pyrrolidine ring. Formation of a six-membered ring intramolecular hydrogen bond $-\text{OH}\cdots\text{N}$ (pyrrolidine) as shown in Figure 13a might be imagined as slightly favored. From the evidence obtained by 2D ^1H – ^1H NOESY, it is also suggested that it is more probable to form the intramolecular hydrogen bond $-\text{OH}\cdots\text{N}$ (oxazine) as depicted in Figure 13b. One of the most common hydrogen-bonding interactions in benzoxazine is the intramolecular $-\text{OH}\cdots\text{N}$.^{35,36} It is not only in polybenzoxazine but also in its monomer if there is a hydrogen bonds donor such as OH.³⁷ All in all, it still needs to be mentioned that most of the OH groups are involved in intramolecular hydrogen bonds either in solid state based on the FT-IR data or in solution state based on the ^1H NMR results. However, there might be small amounts of intermolecular hydrogen bonds between DMSO- d_6 and NN-pd-OH in the solution state. As mentioned before, DMSO is a strong hydrogen-bonding acceptor which can interact with the –OH proton from NN-pd-OH, and it would be able to form intermolecular hydrogen bonds.

Mechanism of the Latent Catalyst Activity. Combining the 2D ^1H – ^1H NOESY NMR results, the mechanism of the latent catalytic effects of the –OH group on the polymerization of NN-pd-OH can now be considered as illustrated in Scheme 2. It is acceptable based on NOESY study that most of the –OH group interacts with pyrrolidine and oxazine ring in such a way that an intramolecular hydrogen bond is formed between OH and N.

Scheme 2. Proposed Mechanism of the Built-in Latent Catalyst Activity for NN-pd-OH

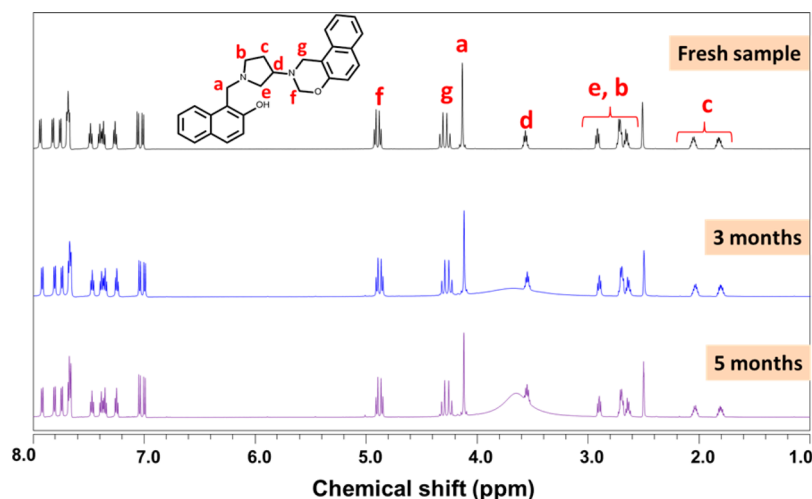
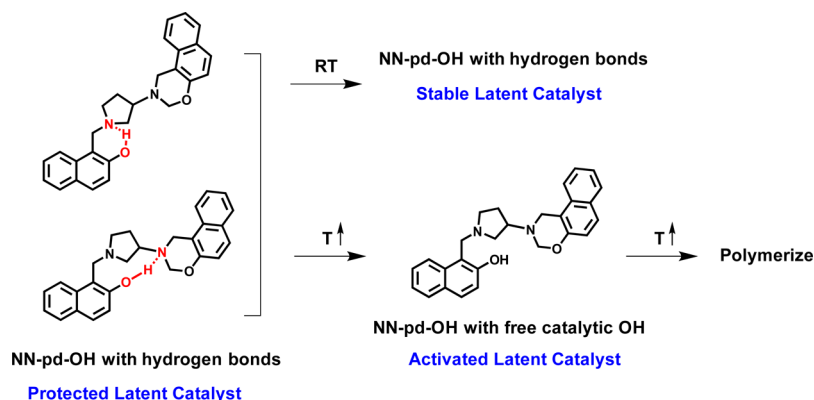


Figure 14. ^1H NMR spectra of NN-pd-OH with a concentration of 70 mM in $\text{DMSO}-d_6$ (in black) and that stored in the dark for 3 months (in blue) and 5 months (in purple).

At room temperature, there is few free catalytic $-\text{OH}$ in this monomeric naphthoxazine since most of them are hydrogen bonded. It is also one of the reasons that this naphthoxazine is stable and has a long shelf life at room temperature as shown in Figure S6, which shows no chemical changes in NN-pd-OH monomer that has been stored in solid state for longer than 3 months. It is noteworthy that the latent catalytic effect in this naphthoxazine is different from the conventional melting-induced or liquid-phase-related latent effect. This latent effect works only if the intramolecular hydrogen bonds are broken at a relatively high temperature, and there is no catalytic effect on ring-opening polymerization at a solution state at room temperature during the storage, distinguishing from melting-induced latent effect. Figure 14 shows ^1H NMR spectra of NN-pd-OH with a concentration of 70 mM in $\text{DMSO}-d_6$ and that stored in the dark for 3 months and up to 5 months. All of the signals for NN-pd-OH have no change even after 5-month storage, which means this OH-containing naphthoxazine monomer is stable even in solution state. That is to say, most of the $-\text{OH}$ group is hydrogen-bonded and protected. It also indicates that NN-pd-OH with a built-in latent catalyst has a long shelf life. The only thing changed in this spectrum is the signal for H_2O (broad peak around 3.7 ppm). As $\text{DMSO}-d_6$ is very easy to absorb water, especially for the extremely dried $\text{DMSO}-d_6$ in this study, the stored sample absorbs moisture from air during the storage. Once the temperature is raised, the

hydrogen bonds in this naphthoxazine are disrupted, generating free $-\text{OH}$, which then becomes active. Finally, the activated $-\text{OH}$ catalyzes the polymerization of this naphthoxazine. The proposed mechanism is illustrated in Scheme 2. It is meaningful to point out that hydrogen bonds act as a protecting group of the catalytic $-\text{OH}$. This is why the system is a latent catalyst with a built-in structure.

CONCLUSIONS

A stable naphthoxazine has been developed by introducing a built-in latent catalyst based on the $-\text{OH}$ group as part of the naphthoxazine monomer. The $-\text{OH}$ group interacts with the two types of N in this naphthoxazine forming intramolecular hydrogen bonds $-\text{OH}\cdots\text{N}$. This built-in latent catalyst in naphthoxazine is stable at room temperature either in solid state or in solution by being protected through the intramolecular hydrogen bonds. It is activated and generates free $-\text{OH}$ as an active latent catalyst by raising temperature and triggers the ring-opening polymerization before the monomer evaporation, minimizing the monomer loss during the polymerization. This ecological approach to achieving the latent catalyst in naphthoxazines shall provide a general platform for naphthoxazines with good stability.

■ ASSOCIATED CONTENT

Supporting Information

The Supporting Information is available free of charge on the ACS Publications website at DOI: 10.1021/acs.macromol.6b01177.

Chemical structures of N-m and 2-naphthol; ^1H NMR spectra of NN-pd-OH before and after adding D_2O ; ^1H NMR spectra of heat-treated NN-pd-OH and N-m/2N (PDF)

■ AUTHOR INFORMATION

Corresponding Authors

*E-mail: hxi3@cwru.edu (H.I.).

*E-mail: pxf106@case.edu (P.F.).

Notes

The authors declare no competing financial interest.

■ ACKNOWLEDGMENTS

W. Zhang gratefully acknowledges the financial support of Chinese Scholarship Council (CSC) Program.

■ REFERENCES

- (1) Nair, C. Advances in Addition-cure Phenolic Resins. *Prog. Polym. Sci.* **2004**, 29, 401–498.
- (2) Ghosh, N. N.; Kiskan, B.; Yagci, Y. Polybenzoxazines—New High Performance Thermosetting Resins: Synthesis and Properties. *Prog. Polym. Sci.* **2007**, 32, 1344–1391.
- (3) Takeichi, T.; Kawauchi, T.; Agag, T. High Performance Polybenzoxazines as a Novel Type of Phenolic Resin. *Polym. J.* **2008**, 40, 1121–1131.
- (4) Ishida, H. Overview and Historical Background of Polybenzoxazine Research. In *Handbook of Benzoxazine Resins*; Ishida, H., Agag, T., Eds.; Elsevier: Amsterdam, 2011; Chapter 1, pp 3–81.
- (5) Takeichi, T. Synthesis and Characterization of Novel Benzoxazine Monomers Containing Allyl Groups and Their High Performance Thermosets. *Macromolecules* **2003**, 36, 6010–6017.
- (6) Ishida, H.; Low, H. Y. A Study on the Volumetric Expansion of Benzoxazine-Based Phenolic Resin. *Macromolecules* **1997**, 30, 1099–1106.
- (7) Ishida, H.; Allen, D. J. Physical and Mechanical Characterization of Near-Zero Shrinkage Polybenzoxazines. *J. Polym. Sci., Part B: Polym. Phys.* **1996**, 34, 1019–1103.
- (8) Chernykh, A.; Agag, T.; Ishida, H. Synthesis of Linear Polymers Containing Benzoxazine Moieties in the Main Chain with High Molecular Design Versatility via Click Reaction. *Polymer* **2009**, 50, 382–390.
- (9) Espinosa, M. A.; Galia, M.; Cadiz, V. Novel Phosphorinated Flame Retardant Thermosets: Epoxy-Benzoxazine-Novolac Systems. *Polymer* **2004**, 45, 6103–6109.
- (10) Hwang, H. J.; Lin, C. Y.; Wang, C. S. Flame Retardancy and Dielectric Properties of Dicyclopentadiene-based Benzoxazine Cured with a Phosphorus-containing Phenolic Resin. *J. Appl. Polym. Sci.* **2008**, 110, 2413–2423.
- (11) Wang, C. F.; Su, Y. C.; Kuo, S. W.; Huang, C. F.; Sheen, Y. C.; Chang, F. C. Low-surface-free-energy Materials Based on Polybenzoxazines. *Angew. Chem., Int. Ed.* **2006**, 45, 2248–2251.
- (12) Dong, H.; Xin, Z.; Lu, X.; Lv, Y. Effect of N-substituents on the Surface Characteristics and Hydrogen Bonding Network of Polybenzoxazines. *Polymer* **2011**, 52, 1092–1101.
- (13) Shen, S. B.; Ishida, H. Synthesis and Characterization of Polyfunctional Naphthoxazines and Related Polymers. *J. Appl. Polym. Sci.* **1996**, 61, 1595–1605.
- (14) Agag, T. Preparation and Properties of Some Thermosets Derived from Allyl-functional Naphthoxazines. *J. Appl. Polym. Sci.* **2006**, 100, 3769–3777.
- (15) Uyar, T.; Koyuncu, Z.; Ishida, H.; Hacaloglu, J. Polymerization and Degradation Processes in Aromatic Amine-based Naphthoxazine; a Pyrolysis Mass Spectrometry Study. *Polym. Degrad. Stab.* **2008**, 93, 2096–2113.
- (16) Ohashi, S.; Pandey, V.; Arza, C. R.; Froimowicz, P.; Ishida, H. Simple and Low Energy Consuming Synthesis of Cyanate Ester Functional Naphthoxazines and Their Properties. *Polym. Chem.* **2016**, 7, 2245–2252.
- (17) Liu, J.; Ishida, H. Anomalous Isomeric Effect on the Properties of Bisphenol F-based Benzoxazines: Toward the Molecular Design for Higher Performance. *Macromolecules* **2014**, 47, 5682–5690.
- (18) Uyar, T.; Hacaloglu, J.; Ishida, H. Synthesis, Characterization, and Thermal Properties of Alkyl-functional Naphthoxazines. *J. Appl. Polym. Sci.* **2013**, 127, 3114–3123.
- (19) Dunkers, J.; Ishida, H. Reaction of Benzoxazine-Based Phenolic Resins with Strong and Weak Carboxylic Acids and Phenols as Catalysts. *J. Polym. Sci., Part A: Polym. Chem.* **1999**, 37, 1913–1921.
- (20) Baqar, M.; Agag, T.; Huang, R.; Maia, J.; Qutubuddin, S.; Ishida, H. Mechanistic Pathways for the Polymerization of Methylol-Functional Benzoxazine Monomers. *Macromolecules* **2012**, 45, 8119–8125.
- (21) Kiskan, B.; Yagci, Y.; Ishida, H. Synthesis, Characterization and Properties of New Thermally Curable Polyetheresters Containing Benzoxazine Moieties in the Main Chain. *J. Polym. Sci., Part A: Polym. Chem.* **2008**, 46, 414–420.
- (22) Kudoh, R.; Sudo, A.; Endo, T. A Highly Reactive Benzoxazine Monomer, 1-(2-Hydroxyethyl)-1,3-Benzoxazine: Activation of Benzoxazine by Neighboring Group Participation of Hydroxyl Group. *Macromolecules* **2010**, 43, 1185–1187.
- (23) Schnell, I.; Brown, S. P.; Low, H. Y.; Ishida, H.; Spiess, H. W. An Investigation of Hydrogen Bonding in Benzoxazine Dimers by Fast Magic-Angle Spinning and Double-Quantum NMR Spectroscopy. *J. Am. Chem. Soc.* **1998**, 120, 11784–11795.
- (24) Kim, H. D.; Ishida, H. A Study on Hydrogen Bonding in Controlled-Structure Benzoxazine Model Oligomers. *Macromol. Symp.* **2003**, 195, 123–140.
- (25) Kuo, S. W.; Wu, Y. C.; Wang, C. F.; Jeong, K. U. Preparing Low-Surface-Energy Polymer Materials by Minimizing Intermolecular Hydrogen-Bonding Interactions. *J. Phys. Chem. C* **2009**, 113, 20666–20673.
- (26) Froimowicz, P.; Zhang, K.; Ishida, H. Intramolecular Hydrogen Bonding in Benzoxazines: When Structural Design Becomes Functional. *Chem. - Eur. J.* **2016**, 22, 2691–2707.
- (27) Steiner, T. The Hydrogen Bond in the Solid State. *Angew. Chem., Int. Ed.* **2002**, 41, 48–76.
- (28) Kim, H. D.; Ishida, H. A Study on Hydrogen-Bonded Network Structure of Polybenzoxazines. *J. Phys. Chem. A* **2002**, 106, 3271–3280.
- (29) Kissinger, H. E. Reaction Kinetics in Differential Thermal Analysis. *Anal. Chem.* **1957**, 29, 1702–1706.
- (30) Ozawa, T. Kinetics of Non-Isothermal Crystallization. *Polymer* **1971**, 12, 150–158.
- (31) Zhang, K.; Ishida, H. An Anomalous Trade-off Effect on the Properties of Smart Ortho-functional Benzoxazines. *Polym. Chem.* **2015**, 6, 2541–2550.
- (32) Baqar, M.; Agag, T.; Ishida, H.; Qutubuddin, S. Polymerization Behavior of Methylol-functional Benzoxazine Monomer. *React. Funct. Polym.* **2013**, 73, 360–368.
- (33) Hassan, W.; Liu, J.; Howlin, B. J.; Ishida, H.; Hamerton, I. Examining the Influence of Bisphenol A on the Polymerisation and Network Properties of an Aromatic Benzoxazine. *Polymer* **2016**, 88, 52–62.
- (34) Freedman, H. H. Intramolecular H-Bonds. I. A Spectroscopic Study of the Hydrogen Bond between Hydroxyl and Nitrogen. *J. Am. Chem. Soc.* **1961**, 83, 2900–2905.
- (35) Dunkers, J.; Zarate, E. A.; Ishida, H. Crystal Structure and Hydrogen-Bonding Characteristics of N,N-Bis(3,5-dimethyl-2-hydroxybenzyl)methylamine, A Benzoxazine Dimer. *J. Phys. Chem.* **1996**, 100, 13514–13520.

- (36) Kim, H.; Ishida, H. A Study on Hydrogen Bonding in Controlled-structure Benzoxazine Model Oligomers. *Macromol. Symp.* **2003**, *195*, 123–140.
- (37) Kim, H.; Ishida, H. A Study on Hydrogen-Bonded Network Structure of Polybenzoxazines. *J. Phys. Chem. A* **2002**, *106*, 3271–3280.